A preconditioned deepest descent algorithm for a class of optimization problems involving the $p(x)$-Laplacian operator*

Sergio González-Andrade
Research Center on Mathematical Modeling (MODEMAT) and
Departamento de Matemática - Escuela Politécnica Nacional
Quito 170413, Ecuador.
sergio.gonzalez@epn.edu.ec

María de los Ángeles Silva
Facultad de Ciencias - Escuela Politécnica Nacional
Quito 170413, Ecuador.
maria.silva@epn.edu.ec

May 24, 2022

Abstract

In this paper we are concerned with a class of optimization problems involving the $p(x)$-Laplacian operator, which arise in imaging and signal analysis. We study the well-posedness of this kind of problems in an amalgam space considering that the variable exponent $p(x)$ is a log-Hölder continuous function. Further, we propose a preconditioned descent algorithm for the numerical solution of the problem, considering a "frozen exponent" approach in a finite dimension space. Finally, we carry on several numerical experiments to show the advantages of our method. Specifically, we study two detailed example whose motivation lies in a possible extension of the proposed technique to image processing.

Keywords: Variable exponent spaces. Amalgam spaces. Finite elements. Optimization problems.

AMS Subject Classification: 65K10. 65N30. 46E30.

1 Introduction

This paper is concerned with the computational solution of the following optimization problem

$$\min_{u\in V^{p(\cdot)}(\Omega)} J(u) := \int_\Omega \frac{1}{p(x)}|\nabla u|^{p(x)}dx + \frac{\lambda}{2}\int_\Omega |u-f|^2 dx, \tag{1}$$

where $V^{p(\cdot)}(\Omega)$ is a suitable space with variable exponent, $\Omega \subset \mathbb{R}^n$ is an open and bounded set, with regular boundary $\partial\Omega$, $\lambda \geq 0$, $p : \Omega \to [1, \infty)$ is a measurable function such that $1 < p(x) \leq 2$ and $f \in L^2(\Omega)$.

*Supported in part by the Escuela Politécnica Nacional del Ecuador, under the project PIGR 19-02.

The $p(x)$-Laplacian operator is a functional extension of the classical Laplacian (when $p(x) \equiv 2$), and the p-Laplacian (if $p(x) \equiv p$, $1 < p < \infty$). The interest in this operator has became relevant in the recent years due to its application in several models related to image processing and electrorheological fluids (see, for instance, [3, 8, 19]).

In order to discuss the theoretical properties of these problems, several authors have focused on the development of variable exponent function spaces and provided a solid background for the study of existence, uniqueness and regularity of solutions. In this regard, we start by citing [13], which is to us the best textbook to understand variable exponent spaces and their main features. In [2], the authors analyse the existence of solutions for the elliptic $p(x)$-Laplacian problem, considering diverse boundary conditions. In [18], the author analyses the existence of solutions for the Dirichlet $p(x)$-Laplacian problem from variational and topological perspectives. In [5], the authors consider the elliptic nonlinear $p(x)$-Laplacian problem and provide several regularity estimates considering specific hypothesis on both the variable exponent p and the associated nonlinearities. It is remarkable the work developed in [1], where the parabolic $p(x)$-Laplacian problem in considered and, furthermore, a class of amalgam spaces is introduced, giving a suitable framework for problems combining functions in variable exponent spaces and usual function spaces.

Regarding the numerical approach to $p(x)$-Laplacian problems, we mention [4], where the authors discuss in detail the finite element discretization of a vector elliptic $p(x)$-Laplacian problem, and introduce the idea of "frozen exponents", which follows from a local approximation of the variable exponent at each triangle of the FEM mesh. The authors obtain optimal approximation estimators for the discretized and the "frozen" problems. However, they do not perform computational experiments in this paper. In [10], the authors also discuss the finite element discretization of the elliptic $p(x)$-Laplacian equation and study the order of convergence for this approximation, providing optimal estimators and computational experiments. Further, in [9], the same authors discuss a discontinuous Galerkin discretization for a similar problem as the one we consider in this paper. They develop a detailed analysis of the approximation and perform one computational experiment for a one dimensional problem.

Considering a computational perspective, we refer [6], where the authors propose an algorithm based on the BFGS method applied to the energy functional associated to the elliptic $p(x)$-Laplacian equation. Here, they carry out several numerical experiments and build benchmark examples for the elliptic Dirichlet problem. In [7], the same authors develop an algorithm based on the inverse power method to compute eigenvalues associated to the $p(x)$-Laplacian operator. They also provide several numerical experiments in diverse geometries.

When discussing the class of problems which are the main concern of this paper, we must start with [8]. In this contribution, the authors introduce a model for image restoration based on a functional involving a variable exponent. They propose the model and develop a concerned theoretical analysis. Further, they propose a computational approach by solving the Euler-Lagrange equations associated to the optimization problem. In [3], the authors extend the model proposed in [8] by considering a more general term for the fidelity term taking a L^q norm instead of a L^2 norm. Also, they develop computational experiments by a similar approach applied to the Euler-Lagrange equations.

In this paper, we propose to study the well posedness of (1) in amalgam spaces. This approach provides a versatile framework to analyse problems which combine terms in variable exponent spaces and terms in usual Lebesgue spaces. In this aim, we adapt the techniques of the direct method in the calculus of variations to the functional defined in a space built taking into account the ideas of [1]. We consider that the proposed theoretical approach is, to the best of our knowledge, a novel way to analyse this kind of problems.

Regarding the computational approximation, we take the discretize-then-optimize approach to

the problem. Thus, we start by proposing a finite element approximation for (1), and we develop a deepest descent algorithm, based on the construction of preconditioned descent directions, for the discretized objective functional. The main idea is to extend the variational and optimization techniques from [14] to the $p(x)$-Laplacian structure. In this aim, we adapt the "frozen exponent" approach from [4] to the present case. Once we have the "frozen problem" defined and analysed, we propose to compute the preconditioned descent directions by solving, iteratively, a variational equation involving a local approximation for the $p(x)$-Laplacian operator. Further, we are able to construct a modular, which can be seen as a weighted norm in the finite element space, to prove that the preconditioned descent directions for the "frozen" problems are indeed descent directions for the objective functional. The main advantage of the proposed method is that each iteration only demands the solution of one linear system of equations involving a weighted system matrix. This fact makes the total computational cost low, specially when compared with other algorithmic tools like quasi-Newton algorithms or the numerical solution of complex systems of PDEs.

The rest of the paper is organized as follows. In the next section we present the variable exponent function spaces and their main properties. We also introduce the amalgam spaces in which we pose the optimization problems. In Section 3, we state the optimization problem and discuss its well posedness in a suitable amalgam space, by using the direct method of calculus of variations. Section 4 is devoted to the development of the preconditioned deepest descent algorithm. Here, we propose the finite element discretization for the problem and discuss the "frozen exponent" approach. Next, we write and briefly analyse the algorithm and its main features. Mainly, we prove that the solution of the variational equation involving the approximation of the $p(x)$-Laplacian operator are in fact descent directions for the objective functional. In Section 5 we carry out three detailed numerical experiments to show the performance of the algorithm. First, we apply our method to the Dirichlet elliptic $p(x)$-Laplacian equation to validate the approach. Then, we show two experiments in 2D to show the ability of the algorithm to recover smooth approximations from noisy functions. Finally, the last section is devoted to the conclusions and research perspectives.

2 Spaces with variable exponent

In this section we introduce the function spaces with variable exponent which we use in the forthcoming analysis, and show several properties of them. Let $\Omega \subset \mathbb{R}^n$ be an open and bounded set, and let $p : \Omega \to [1, \infty]$ be a measurable function, which will be called a variable exponent on Ω. For such a function p, we define the following values

$$p^- := p^-_\Omega := \operatorname*{ess\,inf}_{y\in\Omega} p(y) \text{ and } p^+ := p^+_\Omega := \operatorname*{ess\,sup}_{y\in\Omega} p(y).$$

If $p^+ < \infty$, p is said to be a bounded variable exponent.

Definition 2.1. *Let $\varphi : [0, \infty) \to [0, \infty]$ be a convex and left-continuous function such that $\varphi(0) = 0$, $\lim_{t\to 0^+} \varphi(t) = 0$ and $\lim_{t\to\infty} \varphi(t) = \infty$. This kind of functions are called Φ-functions. Moreover, if $\varphi(t) > 0$, for all $t > 0$, φ is called a positive Φ-function.*

In the context of this work, we are interested in the following Φ-functions (see [13])

$$\tilde{\varphi}_p(t) := \frac{1}{p} t^p \text{ and } \hat{\varphi}_p(t) := t^p,$$

where $1 \le p \le \infty$. Moreover, we set the following convention

$$\tilde{\varphi}_\infty(t) = \hat{\varphi}_\infty(t) = \begin{cases} 0, & \text{if } t \in [0, 1] \\ \infty, & \text{if } t \in (1, \infty). \end{cases}$$

Next, let $p(\cdot)$ be a variable exponent. We define the functions $\widetilde{\boldsymbol{\varphi}}_{p(\cdot)} : \Omega \times [0,\infty) \to [0,\infty]$ and $\widehat{\boldsymbol{\varphi}}_{p(\cdot)} : \Omega \times [0,\infty) \to [0,\infty]$ as follows

$$\widetilde{\boldsymbol{\varphi}}_{p(\cdot)}(x,t) = \tilde{\varphi}_{p(x)}(t) = \frac{1}{p(x)} t^{p(x)} \quad \text{and} \quad \widehat{\boldsymbol{\varphi}}_{p(\cdot)}(x,t) = \hat{\varphi}_{p(x)}(t) = t^{p(x)}.$$

Definition 2.2. *Let $\Omega \subset \mathbb{R}^n$ be an open and bounded set and let p be a variable exponent. We define the Lebesgue space with variable exponent $L^{p(\cdot)}(\Omega)$ to be the space of measurable functions for which the modular*

$$\varrho_{p(\cdot)}(u) := \int_\Omega \widehat{\boldsymbol{\varphi}}_{p(\cdot)}(x, |u(x)|) dx$$

is finite. Further, we equip this space with the following Luxemburg norm

$$\|u\|_{L^{p(\cdot)}(\Omega)} = \inf\{\lambda > 0 \,:\, \varrho_{p(\cdot)}(u/\lambda) \leq 1\}.$$

Theorem 2.3. *(Hölder inequality) Let $p, q, s : \Omega \to [1,\infty]$ be variable exponents such that*

$$\frac{1}{p(x)} + \frac{1}{q(x)} = \frac{1}{s(x)}, \ \text{a.e. in } \Omega.$$

Then,

$$\|fg\|_{L^{s(\cdot)}(\Omega)} \leq 2 \|g\|_{L^{p(\cdot)}(\Omega)} \|g\|_{L^{q(\cdot)}(\Omega)},$$

for all $f \in L^{p(\cdot)}(\Omega)$ and $g \in L^{q(\cdot)}(\Omega)$. Further, in the case $s = p = q = \infty$, we use the convention $\frac{s}{p} + \frac{s}{q} = 1$. In particular, we have that $fg \in L^{s(\cdot)}(\Omega)$

Proof. For a proof, we refer the reader to [13, Lem. 3.2.20]. □

Proposition 2.4. *Let $p : \Omega \to [1,\infty)$ be a variable exponent. Then, for all $w \in L^{p(\cdot)}(\Omega)$, we have that*

$$\sigma^- \left(\|w\|_{p(\cdot)} \right) \leq \int_\Omega |w(x)|^{p(x)} dx \leq \sigma^+ \left(\|w\|_{p(\cdot)} \right), \tag{2}$$

where, for $s \geq 0$, $\sigma^-(s) := \min\{s^{p^-}, s^{p^+}\}$ and $\sigma^+(s) := \max\{s^{p^-}, s^{p^+}\}$.

Proof. For a proof, we refer the reader to [1, Prop. 2.1] and the references therein. □

Definition 2.5. *Let $\Omega \subset \mathbb{R}^n$ be an open and bounded set, and let p be a variable exponent. We define the Sobolev space with variable exponent $W^{1,p(\cdot)}(\Omega)$ as follows*

$$W^{1,p(\cdot)}(\Omega) := \left\{ u \in L^{p(\cdot)}(\Omega) \,:\, \frac{\partial u}{\partial x_i} \in L^{p(\cdot)}(\Omega), \text{ for al } i = 1, 2, \ldots, N \right\}.$$

This space will be equipped with the norm

$$\|u\|_{W^{1,p(\cdot)}(\Omega)} := \left(\|u\|^2_{L^{p(\cdot)}(\Omega)} + \|\nabla u\|^2_{\mathbf{L}^{p(\cdot)}(\Omega)} \right)^{1/2}.$$

Theorem 2.6. *Let $\Omega \subset \mathbb{R}^n$ be an opend and bounded set and let p be a bounded variable exponent. Then, $L^{p(\cdot)}(\Omega)$ and $W^{1,p(\cdot)}(\Omega)$ are separable. Furthermore, if $1 < p^-$ and $p^+ < \infty$, then $L^{p(\cdot)}(\Omega)$ and $W^{1,p(\cdot)}(\Omega)$ are uniformly convex Banach spaces. Consequently, these spaces are reflexive.*

Proof. For a proof, we refer the reader to [13, Sec. 3.4 and Sec 8.1]. □

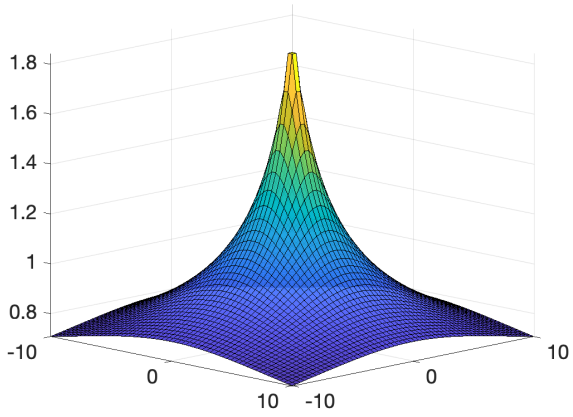

Figure 1: Example of a globally log-Hölder continuous function: $p(x) = c/(\log(e + |x|))$.

Let $p : \Omega \to [0, \infty)$ be a variable exponent. p is said to be log-Hölder continuous if there exists a constant $A > 0$ such that

$$|p(x) - p(y)| \leq \frac{A}{\log(e + 1/|x - y|)}, \quad \text{for all } x, y \in \Omega. \tag{3}$$

This property implies that $p \in C(\overline{\Omega})$ and $p^+ < \infty$ (see [13, p. 100]). In figure 1, we depict the function $p(x) = c/(\log(e + |x|))$, which is globally log-Hölder continuous, with constant $A = c$.

The log-Hölder continuity allows us to have Poincaré and Sobolev inequalities in the spaces with variable exponent. In fact, we have the following result

Definition 2.7. *Let $\Omega \subset \mathbb{R}^n$ be a bounded domain with regular boundary $\partial\Omega$ and let $p : \Omega \to [1, +\infty)$ be a variable exponent which satisfies* (3)*.*

1. *There exists a constant $C \geq 0$ such that*

$$\|u\|_{L^{p(\cdot)}(\Omega)} \leq C\|\nabla u\|_{\mathbf{L}^{p(\cdot)}(\Omega)}, \text{ for all } u \in W_0^{1,p(\cdot)}(\Omega). \tag{4}$$

2. *Let $q : \Omega \to [1, +\infty)$ be a bounded variable exponent, such that*

$$q(x) \leq p^*(x) := \frac{Np(x)}{\max\{0, N - p(x)\}}, \text{ for a.e. } x \in \Omega.$$

Then, $W^{1,p(\cdot)}(\Omega)$ is continuously embedded in $L^{q(\cdot)}(\Omega)$.

The space $W_0^{1,p(\cdot)}(\Omega)$ is defined as the closure of the following set

$$\{w \in W^{1,p(\cdot)}(\Omega) \, : \, u = u\chi_K, \text{ for all compact set } K \subset \Omega\}$$

in the topology of $W^{1,p(\cdot)}(\Omega)$. However, if the variable exponent p satisfies (3), this space is equivalently defined as the closure of $C_0^\infty(\Omega)$ in $W^{1,p(\cdot)}(\Omega)$. This space is usually characterized as the Sobolev space with zero boundary values (see [13, Sec. 8]).

Hereafter, we will use the space $W_0^{1,p(\cdot)}(\Omega)$ under the hypothesis that p is log-Hölder continuous. Hence, we can assume that the Poincaré inequality (4) holds. This fact allows us to equip the space $W_0^{1,p(\cdot)}(\Omega)$ with the following norm

$$\|u\|_{W_0^{1,p(\cdot)}(\Omega)} := \|\nabla u\|_{\mathbf{L}^{p(\cdot)}(\Omega)},$$

which is known to be equivalent with $\|\cdot\|_{W^{1,p(\cdot)}(\Omega)}$.

If we assume that the variable exponent p is log-Hölder continuous, that Ω is bounded and smooth and that $p^- \geq 2N/(N+2)$, there exists a constant $C \geq 0$ such that

$$\|u\|_{L^2(\Omega)} \leq C\|u\|_{W_0^{1,p(\cdot)}(\Omega)}, \text{ for all } u \in W_0^{1,p(\cdot)}(\Omega). \tag{5}$$

See ([1, Prop. 2.2 and pp. 42]).

Note that the structure of the problem (1) and the inequality above suggest the analysis in the following amalgam space with a variable exponent

$$X^{p(\cdot)}(\Omega) := \{u \in L^2(\Omega) \,:\, \partial u/\partial x_i \in L^{p(\cdot)}(\Omega), \text{ for } i = 1, \ldots, N\},$$

equipped with the norm

$$\|u\|_{X^{p(\cdot)}(\Omega)} := \left(\|u\|^2_{L^2(\Omega)} + \|\nabla u\|^2_{\mathbf{L}^{p(\cdot)}(\Omega)}\right)^{1/2}$$

Furthermore, we define the subspace $X_0^{p(\cdot)}(\Omega) \subset X^{p(\cdot)}(\Omega)$ as follows

$$X_0^{p(\cdot)}(\Omega) := X^{p(\cdot)}(\Omega) \cap W_0^{1,p^-}(\Omega),$$

with $\|u\|_{X_0^{p(\cdot)}(\Omega)} = \|u\|_{X^{p(\cdot)}(\Omega)}$. By following [1, p. 42], and by assuming that $1 < p^-$ and $p^+ < \infty$, we can state that both $X^{p(\cdot)}(\Omega)$ and $X_0^{p(\cdot)}(\Omega)$ are reflexive Banach spaces. Moreover, if Ω is assumed to be bounded and regular, we have that

$$W^{1,p^+}(\Omega) \cap L^2(\Omega) \hookrightarrow X^{p(\cdot)}(\Omega) \hookrightarrow W^{1,p^-}(\Omega) \cap L^2(\Omega),$$
$$W_0^{1,p^+}(\Omega) \cap L^2(\Omega) \hookrightarrow X_0^{p(\cdot)}(\Omega) \hookrightarrow W_0^{1,p^-}(\Omega) \cap L^2(\Omega),$$

with continuous injections in both cases.

Proposition 2.8. *Let Ω be an open and bounded set in $\mathbb{R}^n$ with regular boundary $\partial\Omega$. If $p(\cdot)$ is log-Hölder continuous, then $W^{1,p(\cdot)}(\Omega) \cap L^2(\Omega)$ and $W_0^{1,p(\cdot)}(\Omega) \cap L^2(\Omega)$ coincide with $X^{p(\cdot)}(\Omega)$ and $X_0^{p(\cdot)}(\Omega)$, respectively.*

Proof. For a proof, we refer the reader to [1, Prop. 2.4]. □

3 Well-posedness in the amalgam spaces

Once we have introduced the variable exponent spaces, we focus on the well-posedness of the problem (1) in the amalgam space $X_0^{p(\cdot)}(\Omega)$. Therefore, we are concerned with the following problem

$$\min_{u \in X_0^{p(\cdot)}(\Omega)} J(u) := \int_\Omega \frac{1}{p(x)} |\nabla u|^{p(x)} dx + \frac{\lambda}{2} \int_\Omega |u - f|^2 dx. \tag{$\mathcal{P}$}$$

This approach is justified by the structure of the functional J, which combines a term involving a variable exponent and a term in L^2. In order to start with the existence analysis, we present the following Proposition.

Proposition 3.1. *Let p be a variable exponent such that $1 < p^- \leq p(x) < p^+ < 2$. Then, the functional J in $(\mathcal{P})$ is bounded from below and weakly lower semicontinuous (w.l.s.c) in $X_0^{p(\cdot)}(\Omega)$.*

Proof. Let us start by noticing that Proposition 2.4 yields that

$$J(u) \geq \frac{1}{p^+}\sigma^-(||\nabla u_n||_{p(\cdot)}) + \frac{\lambda}{2}||u-f||^2_{L^2(\Omega)} \geq 0,$$

which implies that J is bounded from below. Consequently, it is possible to conclude that there exists $\hat{u} \in X_0^{p(\cdot)}(\Omega)$ such that

$$J(\hat{u}) = \inf_{u \in X_0^{p(\cdot)}(\Omega)} J(u).$$

Next, in order to prove that $J(\cdot)$ is weakly lower semi continuous (w.l.s.c.) in $X_0^{p(\cdot)}(\Omega)$, we write the functional as a sum of the following functionals $\Psi : X_0^{p(\cdot)}(\Omega) \to \mathbb{R}$ and $G : X_0^{p(\cdot)}(\Omega) \to \mathbb{R}$, given by

$$\Psi(u) := \int_\Omega \frac{1}{p(x)}|\nabla u(x)|^{p(x)}dx \quad \text{and} \quad G(u) := \frac{\lambda}{2}\int_\Omega |u-f|^2 dx.$$

We start by showing that $\Psi(u) := \int_\Omega \frac{1}{p(x)}|\nabla u(x)|^{p(x)}dx$ is a continuous functional in $X_0^{p(\cdot)}(\Omega)$. Indeed, let $\{u_k\} \subset X_0^{p(\cdot)}(\Omega)$ be a sequence in $X_0^{p(\cdot)}(\Omega)$ such that $u_k \to u \in X_0^{p(\cdot)}(\Omega)$, as $k \to \infty$. Then, we have that

$$u_k \to u \text{ in } L^2(\Omega) \quad \text{and} \quad \nabla u_n \to \nabla u \text{ in } L^{p(\cdot)}(\Omega). \tag{6}$$

On the other hand, we have that

$$\left|\frac{1}{p(x)}|\nabla u_k(x)|^{p(x)}\right| \leq \frac{1}{p^-}|\nabla u_k(x)|^{p(x)}, \text{ a.e. in } \Omega,$$

which implies, since $\{\nabla u_k\} \in L^{p(\cdot)}(\Omega)$, that $\frac{1}{p^-}|\nabla u_k(x)|^{p(x)} \in L^1(\Omega)$. Finally, thanks to the Lebesgue's dominated convergence theorem, we have that

$$\Psi(u_k) = \int_\Omega \frac{1}{p(x)}|\nabla u_k(x)|^{p(x)}dx \to \int_\Omega \frac{1}{p(x)}|\nabla u(x)|^{p(x)}dx = \Psi(u).$$

Convexity of Ψ in $X_0^{p(\cdot)}(\Omega)$ directly follows from the fact that the application $u \mapsto u^{p(x)}$ is known to be convex for $1 < p^- < p(x) < p^+ \leq 2$ (see [13, Th. 3.4.9]).

Let us now turn our attention to the functional G. First, note that G can be rewritten as

$$G(u) = \frac{\lambda}{2}||u-f||^2_{L^2(\Omega)}.$$

It is clear that this functional is convex in $L^2(\Omega)$, and consequently, in $X_0^{p(\cdot)}(\Omega)$. Next, let $\{u_k\} \subset X_0^{p(\cdot)}(\Omega)$ be a sequence, such that $u_k \to u \in X_0^{p(\cdot)}(\Omega)$, as $k \to \infty$. Thus, thanks to (6), we have that $u_k \to u$ in $L^2(\Omega)$, which directly implies that

$$G(u_k) = \frac{\lambda}{2}||u_k - f||^2_{L^2(\Omega)} \to \frac{\lambda}{2}||u-f||^2_{L^2(\Omega)} = G(u),$$

and the continuity follows.

Summarizing, we have that both Ψ and G are convex and continuous in $X_0^{p(\cdot)}(\Omega)$. Hence, thanks to [20, Th. 2.12], we conclude that Ψ and G are w.l.s.c. in $X_0^{p(\cdot)}(\Omega)$. Finally, thanks to [16, Sec. 1.2.2], we can state that $J(u) = \Psi(u) + G(u)$ is a weakly lower semicontinuous functional in $X_0^{p(\cdot)}(\Omega)$. □

The Lemma above provides the basic elements to complete the existence proof by using the direct method of the calculus of variations. Based on this approach, we have the following existence and uniqueness result

Theorem 3.2. *Let p be a variable exponent such that $1 < p^- < p(x) < p^+ \leq 2$. Then, problem $(\mathcal{P})$ has a unique solution $\bar{u} \in X_0^{p(\cdot)}(\Omega)$.*

Proof. We start by introducing a minimizing sequence $\{u_k\} \subset X_0^{p(\cdot)}(\Omega)$, such that

$$J(u_k) \to J(\hat{u}) = \inf_{u \in X_0^{p(\cdot)}(\Omega)} J(u) \text{ as } k \to \infty.$$

Next, let us show that $\{u_k\}_{n\in\mathbb{N}}$ is bounded in $X_0^{p(\cdot)}(\Omega)$. In fact, note that the Proposition 2.4 and the parallelogram equality imply that

$$\begin{aligned} J(u_k) &\geq \tfrac{1}{p^+}\sigma^-(||\nabla u_k||_{p(\cdot)}) + \tfrac{\lambda}{2}||u_k - f||^2_{L^2(\Omega)} \\ &\geq \tfrac{1}{p^+}\sigma^-(||\nabla u_k||_{p(\cdot)}) + \tfrac{\lambda}{2}||u_k||^2_{L^2(\Omega)} - 2(u_k, f)_{L^2} + \tfrac{\lambda}{2}||f||^2_{L^2(\Omega)}. \end{aligned} \tag{7}$$

On the other hand, we know that $||u||_{X_0^{p(\cdot)}(\Omega)} = (||u||_2^2 + ||\nabla u||^2_{p(\cdot)})^{1/2}$. Thus, if $||u||_{X_0^{p(\cdot)}(\Omega)} \to +\infty$, it follows that $||u||^2_{L^2(\Omega)} \to +\infty$ and/or $||\nabla u_n||^2_{L^{p(\cdot)}(\Omega)} \to +\infty$. Hence, if $||u_k||_{X_0^{p(\cdot)}(\Omega)} \to +\infty$, (7) implies that

$$\lim_{\|u_k\|_{X_0^{p(\cdot)}(\Omega)} \to \infty} J(u_n) = +\infty.$$

Therefore, J is a coercive functional, which implies that the minimizing sequence must be bounded. Further, since J is a w.l.s.c. and coercive functional, [16, Th. 1.5 and Th. 1.6] imply that (1) has a solution $\bar{u} \in X_0^{p(\cdot)}(\Omega)$. Finally, the uniqueness follows from the strict convexity of J. □

4 A Preconditioned Deepest Descent Algorithm

We analyze the numerical solution of problem $(\mathcal{P})$ by a discretize then optimize approach. Thus, we propose a finite element discretization for the problem. Then, let $\mathcal{T}^h$ be a regular triangulation, in the sense of Ciarlet, of Ω. Next, let Ω^h be a polygonal approximation of Ω, given by $\Omega^h := \cup_{\tau\in\mathcal{T}^h}\overline{\tau}$, where all the open disjoint regular triangles have maximum diameter bounded by h. Further, for any two triangles, their closures are either disjoint or have a common vertex or a common side. Finally, let $\{P_j\}_{j=1,\ldots,N}$ be the vertices associated with the triangulation $\mathcal{T}^h$. Hereafter, we assume that $P_j \in \partial\Omega^h$ implies that $P_j \in \partial\Omega$ and that $\Omega^h \subset \Omega$.

On the other hand, thanks to (5) and Proposition 2.8, and since $N = 2$ and p is assumed to be log-Hölder continuous, we can conclude that $X_0^{p(\cdot)}(\Omega)$ coincide with $W_0^{1,p(\cdot)}(\Omega)$ (see, also, [1, pp. 47]). Therefore, we propose the finite element approximation in this space. In this aim, by following [4], we define the finite dimension space $X_0^h \subset W_0^{1,p(\cdot)}(\Omega)$, as follows

$$X_0^h := V_h \cap W_0^{1,p(\cdot)}(\Omega), \text{ with } V_h := \{v \in L^1_{loc}(\Omega) \,:\, v|_\tau \in \mathbb{P}_1\}.$$

Here, $\mathbb{P}_1$ is the space of polynomials with degree at most 1. In this paper we will only consider first order approximation, since the solutions of the p-Laplacian type problems usually exhibit limited higher order regularity (see [6, 17] and the references therein).

Considering the discussion above, we introduce the discretized optimization problem as follows

$$\min_{u_h \in X_0^h} J_h(u_h) := \int_\Omega \frac{1}{p(x)} |\nabla u_h|^{p(x)} dx + \frac{\lambda}{2} \int_\Omega |u_h - f|^2 dx. \tag{$\mathcal{P}^h$}$$

Since p is a log-Hölder continuous function, considering the results in [4], it is possible to state that the discretized problem has a unique solution. Indeed, the direct application of a similar argumentation as the one used in Section 3, considering that X_0^h is a closed subspace of $W_0^{1,p(\cdot)}(\Omega)$, yields the existence of a unique solution for the discretized problem ($\mathcal{P}^h$).

4.1 Frozen exponents

We propose to use the technique of frozen exponents developed in [4]. The main idea is to propose a local approximation of the variable exponent and use this approximation in the discretized functional. In this aim, we use a simple weighting operator to obtain the value of the function p in the gravity center x_τ of each triangle $\tau \in \mathcal{T}^h$, obtaining the following

$$p_{\mathcal{T}}(x) := \sum_{\tau \in \mathcal{T}^h} p(x_\tau) \chi_\tau(x)$$

Once we have this local approximation for the variable exponent, we focus on the following problem

$$\min_{u_h \in X_0^h} J_{h,\mathcal{T}}(u_h) := \int_\Omega \sum_{\tau \in \mathcal{T}^h} \chi_\tau(x) \frac{1}{p(x_\tau)} |\nabla u_h|^{p(x_\tau)} \, dx + \frac{\lambda}{2} \int_\Omega |u_h - f|^2 \, dx. \tag{$\mathcal{P}^h_{\mathcal{T}}$}$$

Next, in [4, Rem. 4.7] it is stated that $\|\cdot\|_{p(\cdot)}$ and $\|\cdot\|_{p_{\mathcal{T}}(\cdot)}$ are equivalent on any finite element space, hence on X_0^h. This result guarantees the existence of a unique solution for ($\mathcal{P}^h_{\mathcal{T}}$). Furthermore, by following [4, Th. 4.9] and considering that $p \in C^{0,\alpha}(\overline{\Omega})$ with $p^- > 1$, it would be possible to obtain the following estimator

$$\|J'_{h,\mathcal{T}}(u_h) - J'_{h,\mathcal{T}}(\overline{u}_h)\|_2 \leq c h^\alpha,$$

where $\overline{u}$ is the solution of problem ($\mathcal{P}^h$) and

$$J'_{h,\mathcal{T}}(u_h) v_h := \int_\Omega \sum_{\tau \in \mathcal{T}^h} \chi_\tau(x) |\nabla u_h|^{p(x_\tau)-2} \nabla u_h \cdot \nabla v_h \, dx + \lambda \int_\Omega (u_h - f) v_h \, dx. \tag{8}$$

We will assume that all the previous results hold, so we propose our computational approach for the problem ($\mathcal{P}^h_{\mathcal{T}}$).

4.2 A preconditioned descent direction

The computational approach that we propose for problem ($\mathcal{P}^h_{\mathcal{T}}$) is based on the construction of descent directions by solving, iteratively, the following variational equation

$$\int_\Omega \sum_{\tau \in \mathcal{T}^h} \chi_\tau(x) (\varepsilon + |\nabla u_h|)^{p(x_\tau)-2} \nabla w_h \cdot \nabla v_h \, dx = -J'_{h,\mathcal{T}}(u_h) v_h, \text{ for all } v_h \in X_0^h. \tag{9}$$

We state that the solution w_h is a descent direction for the functional $J_{h,\mathcal{T}}(u_h)$. In fact, we start this discussion by introducing the following expression in X_0^h

$$\varrho_u^h(w^h) := \int_\Omega \left(\sum_{\tau \in \mathcal{T}^h} \chi_\tau(x) (\varepsilon + |\nabla u_h|)^{p(x_\tau)-2} \right) |\nabla w_h|^2 \, dx. \tag{10}$$

It is not difficult to prove that $\varrho_u^h(w^h)$ is a modular in X_0^h, according to [13, Def. 2.1.1]. Particularly, we have that

$$\varrho_u^h(w_h) > 0, \text{ for all } w_h \in X_0^h, \quad \text{and} \quad \varrho_u^h(w_h) = 0, \text{ iff } w_h = 0.$$

Therefore, if we take $v_h = w_h$ in (9), we have that

$$-J'_{h,\mathcal{T}}(u_h)w_h = \int_\Omega \left(\sum_{\tau \in \mathcal{T}^h} \chi_\tau(x)(\varepsilon + |\nabla u_h|)^{p(x_\tau)-2} \right) |\nabla w_h|^2 \, dx = \varrho_u^h(w_h) > 0,$$

which yields that w_h is, indeed, a descent direction for $J_{h,\mathcal{T}}(u_h)$.

Remark 4.1. Existence and uniqueness of solutions for the equation (9) can be analyzed by using the ideas in [14] or [17]. This implies either the construction of a Hilbert subspace in X_0^h in which the modular $\varrho_u^h(w_h)$ acts as a induced norm, or the analysis of the modular as a weighted norm in X_0^h. This analysis, however, is in our consideration out of the scope of the present work. We will resume this discussion in future contributions focused on the development of mesh independent algorithms for problems involving the $p(x)$-Laplacian.

Summarizing, we propose the following preconditioned deepest descent algorithm for the problems under study

Algorithm 4.2. (Preconditioned-DDA)
Define the parameters ε, λ and *tol*. Further, set f, initialize $u_0 \in X_0^h$ and set $k = 0$.
For $k = 1, 2, \ldots$

1. If $J'_{h,\mathcal{T}}(u_h) = 0$, STOP.

2. Find a descent direction $w_h \in X_0^h$ by solving

$$\int_\Omega \sum_{\tau \in \mathcal{T}^h} \chi_\tau(x)(\varepsilon + |\nabla u_h^k|)^{p(x_\tau)-2} \nabla w_h^k \cdot \nabla v_h \, dx = -J'_{h,\mathcal{T}}(u_h^k)v_h, \text{ for all } v_h \in X_0^h. \tag{11}$$

3. Perform an efficient line search technique to obtain the step length $\alpha_k > 0$.

4. Update $u_h^{k+1} := u_h^k + \alpha_k w_h^k \in X_0^h$ and set $k = k + 1$.

Remark 4.3. The convergence of the Algorithm (P-DDA) follows by extending the ideas in [14]. In fact, let us point out that $J_{h,\mathcal{T}}(u_h)$ is a convex and differentiable functional on X_0^h and that w_h is a descent direction. Thus, if we consider a line search algorithm satisfying the Wolfe-Powell conditions, [14, Prop. 13 and Th. 14] guarantee the global convergence of the algorithm.

5 Numerical Results

In this section, we carry out several numerical experiments to show the main features of the proposed method. In order to validate the approach, we first study the behavior of the method in the homogeneous Dirichlet problem for the $p(x)$-Laplacian. Next, we perform the computational solution of $(\mathcal{P}_{\mathcal{T}}^h)$.

Let us make some remarks on the implementation of our algorithm. We stop the Algorithm (P-DDA) as soon as the expression $\frac{\|J'(u_h^k)\|}{\|J'(u_h^0)\|}$ is reduced by a factor of 10^{-6}. This stopping criteria is common to be used when working with descent algorithms and has proved to be computationally optimal (see [14]).

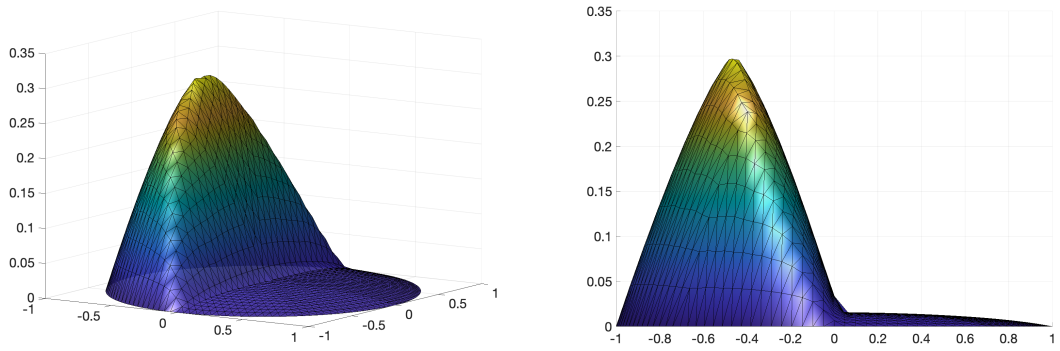

Figure 2: $p(x)$-Poisson equation.

Regarding the line search algorithm, we work with an algorithm which uses polynomial models of the objective functional for backtracking. This algorithm was first proposed in [12], and it was successfully adapted to this class of preconditioned descent algorithms in [14, 15]. The advantage is that this line search technique is known to be efficient and fulfills the Wolfe-Powell conditions. Therefore, it allows us to guarantee the global convergence of the Algorithm (P-DDA). For further details, we refer the reader to [14, Sec. 4.2], and the references therein.

Finally, let us point out that, due to the proposed structure, the Algorithm (P-DDA) only needs to solve one linear system at each iteration. In fact, the Algorithm demands the solution, at every iteration, of a linear systems $A^h_{\varepsilon,u} w^k_h = \eta_h$, where $A^h_{\varepsilon,u}$ corresponds to the finite element implementation of $\int_\Omega \sum_{\tau\in\mathcal{T}^h} \chi_\tau(x)(\varepsilon + |\nabla u^k_h|)^{p(x_\tau)-2}\,\nabla w^k_h \cdot \nabla v_h\,dx$ in (11) and η_h corresponds to the FEM approximation of $-J'_{h,\mathcal{T}}(u^k_h)v_h$. Note that the matrix $A^h_{\varepsilon,u}$ depends on u^k_h, but does not depend on w^k_h, which makes the solution of the system fully accessible with any direct or iterative method. Consequently, we can state that the computational cost of our approach is low.

5.1 The $p(x)$-Poisson equation

In this section, we discuss the application of our proposed method to the following $p(x)$-Laplacian elliptic problem

$$\begin{cases} -\mathrm{div}(|\nabla u(x)|^{p(x)-2}\nabla u(x)) = f(x) & \text{in } \Omega \\ u(x) = 0 & \text{on } \partial\Omega. \end{cases} \tag{12}$$

Here, $\Omega \subset \mathbb{R}^n$ is an open and bounded domain with regular boundary $\partial\Omega$. It is known that the solutions for (12) is characterized as the solution of the following optimization problem (see [6])

$$\min_{u_h\in V^h_0} \tilde{J}(u_h) := \int_\Omega \frac{1}{p(x)}|\nabla u_h|^{p(x)}\,dx - \int_\Omega f u_h\,dx,$$

where $X^h_0 \subset W^{1,p(x)}_0(\Omega)$. Therefore, we propose to apply the Algorithm 4.2 to this optimization problem.

Here, we consider that $\Omega = B_1((0,0))$ and the following variable exponent

$$p(x) = \begin{cases} p^+ & \text{if } x < -0.01 \\ p^- + (p^- - p^+)\frac{x-0.01}{0.02} & \text{if } |x| \le 0.01 \\ p^- & \text{if } x > 0.01. \end{cases}$$

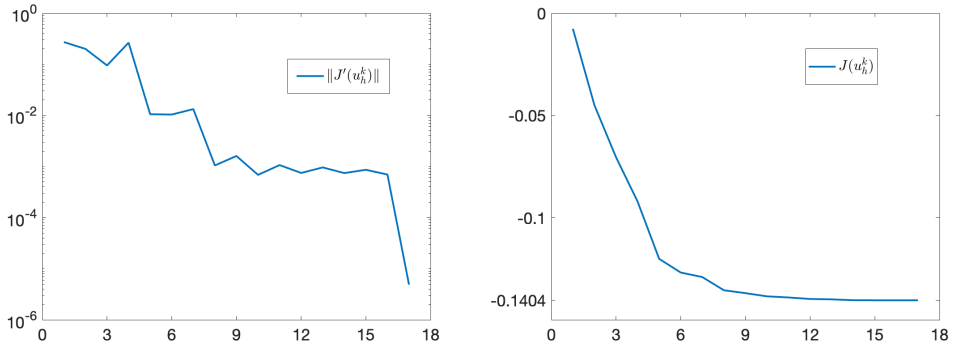

Figure 3: Convergence history for tthe $p(x)$-Poisson equation.

By following [6], we set $f = 1$ and consider that $p^+ = 4$ and $p^- = 1.1$. Further, we use a uniform mesh with $h = 0.0086$. In Figure 2, we depict the calculated solution u, which is in good agreement with the computed solution in [6, Fig. 3]. Further, in Figure 3, we show two pictures to depict the convergence behaviour of the algorithm. In the left picture, the evolution of $\frac{\|J'(u_h^k)\|}{\|J'(u_h^0)\|}$, in each iteration, is depicted. It is possible to see a fast decrease in the last iterations, which indicates that the algorithm reaches a stationary point. This fact is also verified with the evolution of $J(u_h^k)$, which is shown in the image on the right. The value of the objective functional reaches a fixed value that does not improve.

# it.	$\frac{\|J'(u_h^k)\|}{\|J'(u_h^0)\|}$	$J(u_h^k)$
13	9.5988e-4	-0.1400
14	7.4323e-4	-0.1404
15	8.6318e-4	-0.1404
16	6.9567e-4	-0.1404
17	4.8745e-6	-0.1404

Table 1: Convergence history for the $p(x)$-Poisson equation.

Finally, in Table 1 we show the behavior of $\frac{\|J'(u_h^k)\|}{\|J'(u_h^0)\|}$ and $J(u_h^k)$ to summarize the argument discussed above.

5.2 Computational solution of problem $(\mathcal{P}_{\mathcal{T}}^h)$

In this section we are concerned with the computational solution of problem $(\mathcal{P}_{\mathcal{T}}^h)$. We consider that $\Omega = B_1((0,0))$ and $f := u_e + \xi$, where ξ represents a level of Gaussian noise and u_e is the "exact" function to be recovered. In the following experiments, u_e stands for the solution of the following problem

$$\begin{cases} -\Delta u &= \frac{\sqrt{\beta}}{\alpha} \exp\left(\frac{\alpha(x+y+\beta)+\beta}{\beta}\right), & \text{in } \Omega \\ u &= 0, & \text{on } \partial\Omega. \end{cases}$$

We focus on the response of the Algorithm (P-DDA) to different levels of noise and to the value of the parameter λ, which is known to play a key role in the denoising strategy ([8]). In this section

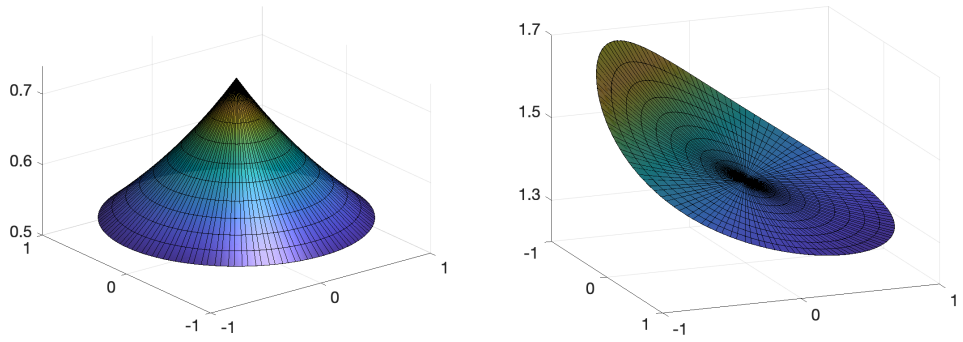

Figure 4: Variable exponents $p_1((x,y))$ (left) and $p_2((x,y))$ (right)

we will work with the following variable exponents (see Figure 4)

$$p_1((x,y)) := \frac{2}{\log(e+\sqrt{x^2+y^2})} \quad \text{and} \quad p_2((x,y)) := 1 + \left(\frac{b}{a}(x+y) + 1 + b\right)^{-1}, \text{ with } a, b \in \mathbb{R}^+.$$

5.2.1 Experiment 1

In this experiment, we consider the variable exponent $p_1((x,y))$. This variable exponent is known to be log-Hölder continuous. Further, it is clear that $1 < p(x) < 2$, for all $x \in \Omega$.

In Figure 5 we show the exact function u_e (left column), the noisy version $u_e+\xi$ (central column) and the computed function u (right column), for different values of the parameter λ: $\lambda = 500$ (upper row), $\lambda = 1000$ (central row) and $\lambda = 10000$ (lower row). For this experiment, we consider a level of 10% of Gaussian white noise, given by ξ. In Figure 6, we show the comparison between the three functions along the diameter of the domain. As depicted, the that the Algorithm (P-DDA) is able to recover a smooth approximation for the function u_e, from the noisy version given by $f = u_e + \xi$, for several values of the parameter λ.

In Table 2, we show the convergence behaviour of the Algorithm (P-DDA) for the different values of the parameter λ. We can observe a monotone decrease in the two approximation estimators: the modular $\int_\Omega \frac{1}{p(x)}|\nabla(u_e-u)|^{p(x)}\,dx$ (which provides a good image of the behaviour of $\|u_e-u\|_{W_0^{1,p(\cdot)}(\Omega)}$) and $\|u_e - u\|_\infty$. Also, the value of the objective functional $J(u_h^k)$ decreases at each iteration. Regarding the convergence, for $\lambda = 500$, we see an oscillatory behaviour of the estimator $\frac{\|J'(u_h^k)\|}{\|J'(u_h^0)\|}$, though decreases in the last iterations. For the other considered values of λ, we see a monotone decrease of this error estimator, at least in the last iterations. It is clear the impact of the parameter λ in the behaviour of the algorithm, mainly in the computational performance.

5.3 Experiment 2

In this experiment, we compare the behaviour of Algorithm (P-DDA) when facing increased amount of Gaussian noise, considering two variable exponents and a fix value for the parameter λ. Here, we do not use the stopping criteria, but allow the algorithm to loop for 40 iterations, at each setting.

In Figures 7 and 8, we show the noisy function $u_e + \xi$, the computed function u and the comparison between u_e, u and $u_e + \xi$ along the diameter of the domain, considerign two levels of noise: 20% in the upper row and 30% in the lower one, for $p_1((x,y))$ and for $p_2((x,y))$, respectively.

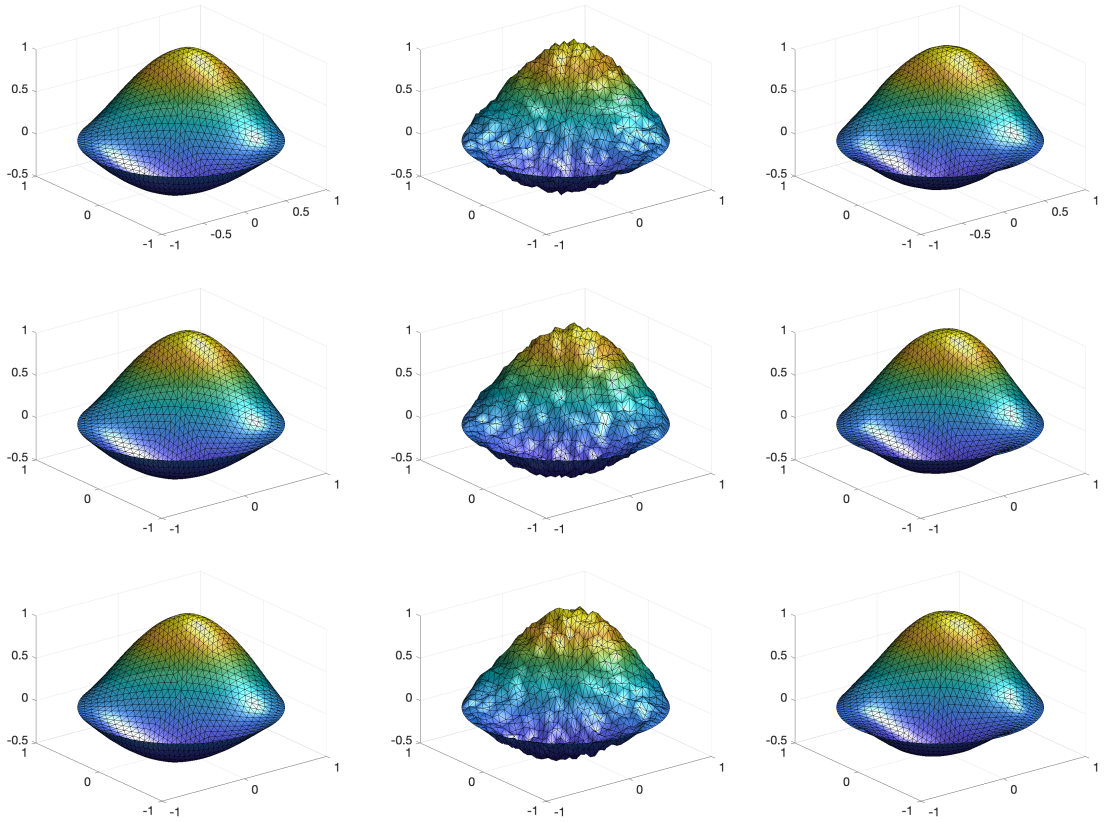

Figure 5: Experiment 1. u_e (left column), $u_e+\xi$ (central column) and u (right column), for $\lambda = 500$ (upper row), $\lambda = 1000$ (central row) and $\lambda = 1e4$ (lower row). Parameters: $\xi = 10\%$

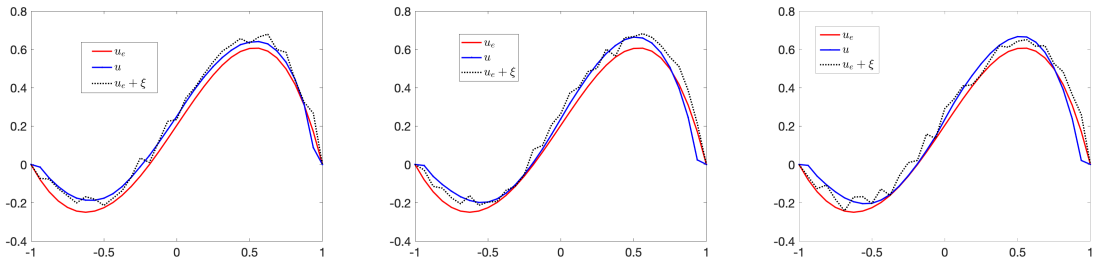

Figure 6: Experiment 1: Comparison between u_e, $u_e + \xi$ and u, with $\xi = 10\%$

λ	# iter	$\int_\Omega \frac{1}{p(x)}\lvert\nabla(u_e-u)\rvert^{p(x)}\,dx$	$\lVert u_e-u\rVert_\infty$	$\frac{\lVert J'(u_h^k)\rVert}{\lVert J'(u_h^k)\rVert}$	$J(u_h^k)$
	7	0.2164	0.1341	2.6526e-5	3.4168
	8	0.1878	0.1255	8.10808e-6	3.3147
	9	0.1902	0.1185	1.6043e-5	3.2459
500	10	0.1774	0.1110	3.5577e-6	3.2004
	11	0.1740	0.1050	1.0317e-5	3.1667
	12	0.1672	0.0985	9.5530e-7	3.1433
	1	1.1093	1.1222	0.0021	48.0430
	2	0.4698	0.4835	6.5475e-4	14.7671
	3	0.3947	0.4096	0.0181	8.5441
1000	4	0.2861	0.3002	0.0045	6.4106
	5	0.2689	0.2812	9.9769e-4e-5	5.3318
	6	0.2181	0.2289	3.5966e-7	4.7008
	1	1.1132	0.3445	2.1143e-4	4.5907e+2
	2	0.4769	0.1737	6.6403e-5	1.2143e+2
	3	0.4072	0.1955	0.0183	5.9583e+1
1e4	4	0.2988	0.1651	0.0045	3.8581e+1
	5	0.2815	0.1559	7.3930e-4e-5	2.8093e+1
	6	0.2291	0.1504	7.4860e-8	2.1889e+1

Table 2: Convergence history for Experiment 1.

In both cases it is possible to appreciate the ability of the Algorithm (P-DDA) for recovering a smooth approximation to u_e from the noisy version $u_e + \xi$. Clearly, if the noise increases, the algorithm faces more difficulties to build the approximated version of u_e. However, the smoothing effect of the optimization algorithm suggests that this algorithm could perform well in multigrid structures or similar approaches. Further, we consider a relatively low value for λ, since for larger values of this parameter, the algorithm tends to perform in an unstable way. These facts suggest to analyse a strategy with an adaptive functional parameter λ which can improve the approximation locally in the whole region. This approach will be studied in future contributions.

$p(x)$	$\%\xi$	$\int_\Omega \frac{1}{p(x)}\lvert\nabla(u_e-u)\rvert^{p(x)}\,dx$	$\frac{\lVert J'(u_h^k)\rVert}{\lVert J'(u_h^k)\rVert}$	$J(u_h^k)$
	20%	0.2858	8.8363e-7	3.0261
$p_1((x,y))$	30%	0.5276	1.1499e-6	2.6157
	20%	0.4535	2.8573e-6	2.7926
$p_2((x,y))$	30%	0.7199	1.6626e-6	3.1046

Table 3: Experiment 2: Estimators after 40 iterations of algorithm P-DDA.

Finally, in Table 3 and Figure 9, we show some final features regarding the convergence of the Algorithm (P-DDA). In the figure, we depict the evolution of the value of the objective functional $J(u_h^k)$ at each iteration, for the two variable exponents and the two considered levels of noise. It is clear that the value of the objective functional reaches a fixed value, suggesting that the algorithm reaches a stationary point (which, due to the convexity of J is actually a minimum). This assertion is confirmed in Table 3, where it is possible to see that $\frac{\lVert J'(u_h^k)\rVert}{\lVert J'(u_h^k)\rVert}$ converges to zero.

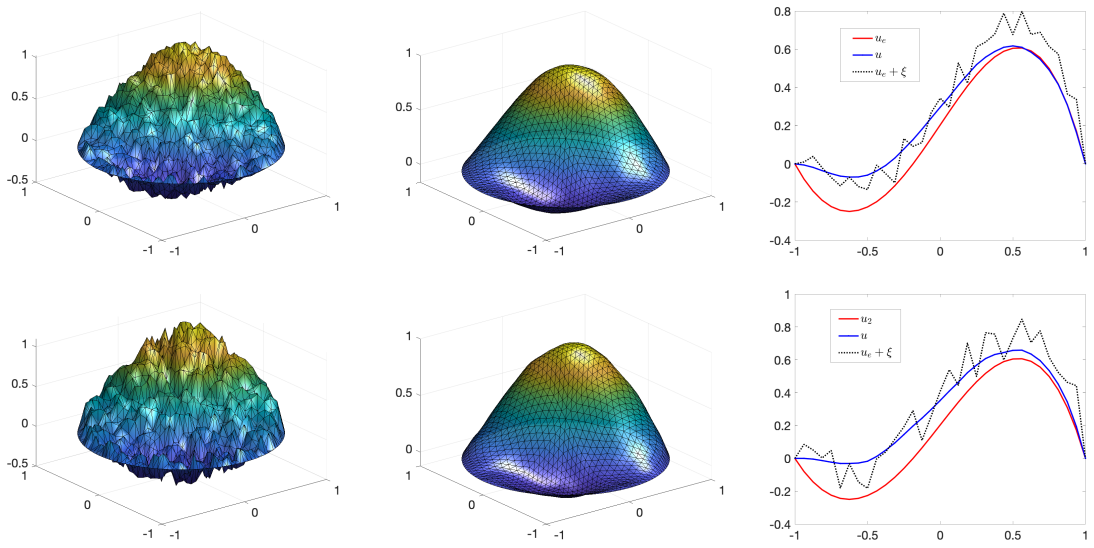

Figure 7: Experiment 2. $u_e + \xi$ (left column), u (right column) and the comparison between u_e, $u_e + \xi$ and u along the diameter of the domain, for $\xi = 20\%$ (upper row), and $\xi = 30\%$ (lower row). Variable exponente $p_1((x, y))$. Parameters: $\lambda = 50$.

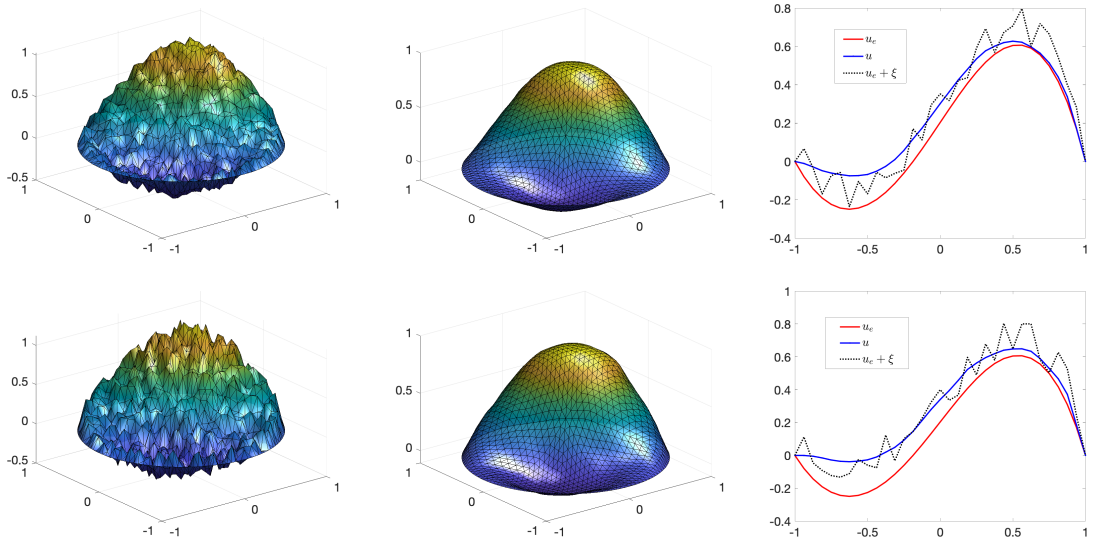

Figure 8: Experiment 2. $u_e + \xi$ (left column), u (right column) and the comparison between u_e, $u_e + \xi$ and u along the diameter of the domain, for $\xi = 20\%$ (upper row), and $\xi = 30\%$ (lower row). Variable exponente $p_2(x, y))$. Parameters: $\lambda = 50$.

6 Conclusions and outlook

We analysed a class of optimization problems, involving the $p(x)$-Laplacian operator, which usually arise in the analysis of signals and imaging. We studied the well posedness of the problem

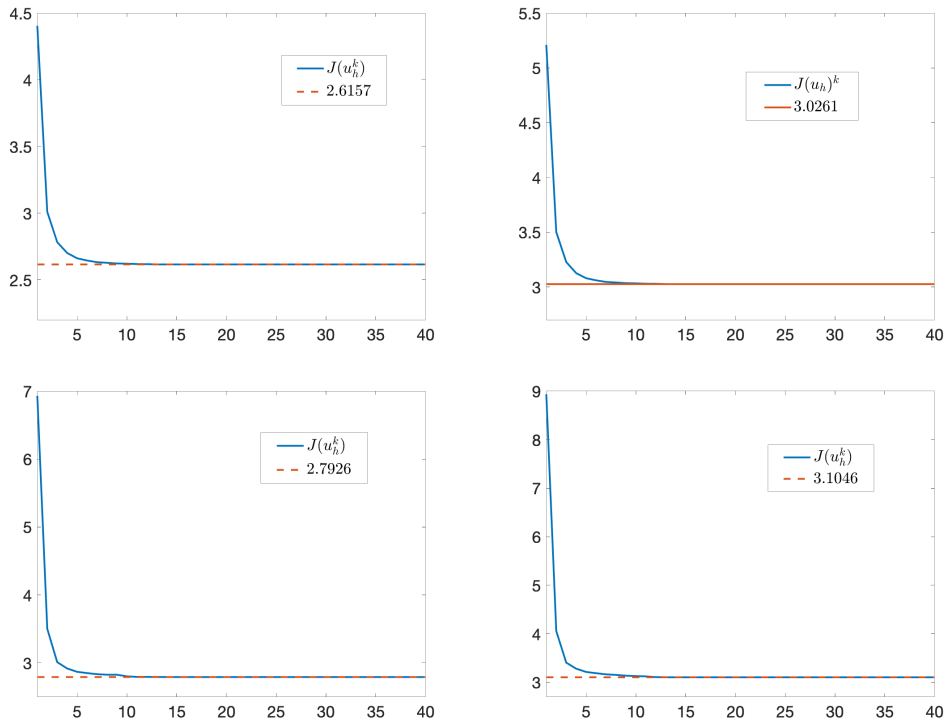

Figure 9: Experiment 2. Evolution of the objective functional for $p_1((x,y))$ (upper row) at $\xi = 20\%$ (left) and $\xi = 30\%$ (right), and for $p_2((x,y))$ (lower row) at $\xi = 20\%$ (left) and $\xi = 30\%$ (right). Parameters: $\lambda = 50$

in an amalgam space, which provides a suitable framework for the analyzed problems, considering the local and the non-local behaviour of the involved functions. We developed a finite element discretization for the problem and extended the "frozen exponents" approach to the discretized problem. Next, we proposed and implemented a preconditioned deepest descent algorithm, based on the construction of preconditioned descent directions which are solutions of variational equations involving the frozen exponent modulars. Finally, we carried out three numerical experiments showing the main features of the algorithm.

In future contributions, we will focus on the application of the proposed methodology to imaging and denoising problems. Mainly, we are interested in the bilevel approach with a functional parameter λ. We also consider that the study of multigrid and multilevel type algorithms is a field worth to explore. The smoothing ability of the algorithm suggest to go this way. This work could be of great interest in the electrorheological fluids simulation, regarding the large-scale systems that usually arise when solving this kind of problems.

References

[1] G. Akagi and K. Matsuura, *Nonlinear difussion equations driven by the $p(\cdot)$-Laplacian*, Nonlinear Differential Equations and Applications, 20 (2012) 37-64.

[2] M. Allaoui, A. El Amrouss and A. Ourraoui, *Existence and uniqueness of solution for $p(x)$-Laplacian problems*, Bol. Soc. Paran. Mat., 30 (2015) 225-232.

[3] E. M. Bollt, R. Chartrand, S. Esedoḡlu, P. Schultz and K. R. Vixie, *Graduated adaptive image denoising: local compromise between total variation and isotropic diffusion*, Adv. Comput. Math., 31 (2009) 61–85

[4] D. Breit, L. Diening and S. Schwarzacher, *Finite element approximation of the $p(\cdot)$-Laplacian*, SIAM J. Numer. Anal. , 53 (2015) 551-572.

[5] Sun-Sig Byun and J. Ok, *On $W^{1,q(\cdot)}$-estimates for elliptic equations of $p(x)$-Laplacian type*, Journal de Mathématiques Pures et Appliquées, 106 (2016) 512-545.

[6] M. Caliari and S. Zuccher, *Quasi-Newton minimization for the $p(x)$-Laplacian problem*, Journal of Computational and Applied Mathematics, 309 (2017) 122-131.

[7] M. Caliari and S. Zuccher, *The inverse power method for the $p(x)$-Laplacian problem*, SIAM J. APPL. MATH., 66 (2006) 1383–1406.

[8] Y. Chen, S. Levine and M. Rao, *Variable exponent, linear growth functionals in image restoration*, Journal of Scientific Computing, 65 (2015) 698–714.

[9] L. Del Pezzo, A. L. Lombardi and S. Martínez, *Interior penalty discontinuous Galerkin FEM for the $p(x)$-Laplacian,* SIAM J. Numer. Anal. , 50 (2012) 2497–2521.

[10] L. Del Pezzo, A. L. Lombardi and S. Martínez, *Order of convergence of the finite element method for the p(x)-Laplacian*, IMA Journal of Numerical Analysis, 35 (2015) 1864–1887.

[11] L. Del Pezzo and S. Martínez, *The decomposition-coordination method for the $p(x)$-Laplacian*, arXiv:1401.2442.

[12] J. E. Dennis and R. B. Schnabel, *Numerical Methods for Unconstrained Optimization and NonlinearEquations*. SIAM, Philadelphia, 1996.

[13] L. Diening, P. Harjulehto, P. Hästo and M. Ruzicka, *Lebesgue and Sobolev spaces with variable exponents*. Springer, Verlag, Heidelberg, 2011.

[14] S. González-Andrade, *A Preconditioned Descent Algorithm for Variational Inequalities of the Second Kind Involving the p-Laplacian Operator*. Computational Optimization and Applications, 66 (2017) 123-162.

[15] S. González-Andrade and S. López-Ordóñez, *A Multigrid Optimization Algorithm for the Numerical Solution of Quasilinear Variational Inequalities Involving the p-Laplacian*. Computers and Mathematics with Applications, 75 (2018) 1107-1127

[16] M. R. Grossinho and S. Agop Tersian, *An Introduction to Minimax Theorems and Their Applications to Differential Equations*. Springer, U.S.A., 2001.

[17] Y. Q. Huang, Ruo Li and Wenbin Liu, *Preconditioned Descent Algorithms for p-Laplacian*. Journal of Scientific Computing, 32 (2007) 343-371.

[18] P. S. Ilias, *Dirichlet problem with $p(x)$-laplacian*. Math. Reports, 10 (2008) 43–56.

[19] M. Růžička, *Electrorheological Fluids: Modeling and Mathematical Theory*. Springer Verlag, Berlin, 2000.

[20] F. Tröltzsch, *Optimal Control of Partial Differential Equations. Theory, Methods and Applications*. AMS, U.S.A., 2010.